BUTTERWORTH HEINEMANN

Thermodynamic models of wet-snow accretion: axial growth and liquid water content on a fixed conductor

G. Poots and P. L. I. Skelton
Centre for Industrial Applied Mathematics, University of Hull, Hull, UK

For wet-snow accretion on overhead line conductors, occurring at positive air temperatures, the liquid water content of the snow matrix controls the strength of the capillary forces, promoting contact between ice granules, which leads to ice bonding. During this process of metamorphosis, the liquid water content of the snow matrix increases with time and, on reaching a level of 20–40 percent, the internal cohesive forces are greatly weakened, causing shedding of the accreted snow by aerodynamic and gravitational forces. The purpose of this paper is to construct thermodynamic models of wet-snow accretion, by axial growth on a fixed conductor, which estimate the liquid water content during the accretion process. The models depend upon assumptions concerning the wet-snow accretion factor, namely the proportion of mass of a snowflake that adheres on impact with the snow/conductor surface. Models are formulated assuming either that the accretion factor is constant or that it obeys a cosine law (adhesion proportional to the cosine of the angle between the impacting snowflake trajectory and the normal to the surface). A differential equation governing the variation of the liquid water content with deposit time is derived and solved numerically. Solutions of this equation are also obtained using analytical solutions of the evolution equation based on the assumption that the trajectory paths of snowflakes are rectilinear. For a range of meteorological conditions, critical cohesive "precipitation—air temperature" criteria are established for wet-snow shedding, leading to quantitative information on the sawtooth transient wet-snow loading of an overhead line conductor.

Keywords: overhead power conductors; wet snow

Introduction

Wet-snow accretion occurs on overhead line conductors at air temperatures just above freezing. When a snowflake, which is a mixture of air, water, and ice at fusion temperature, hits the conductor/snow surface it may fragment, with some of the fragments adhering to the conductor and the remainder ricocheting into the airstream (see Wakahama et al. 1977). During the accretion process, the wet snow undergoes a rapid process of metamorphosis in which the fragments form a snow matrix, held together by capillary forces and ice bonding. The strength of these internal forces depends upon the liquid water content (LWC) of the snow matrix. Admirat et al. (1998a) suggest that if the LWC is greater than 40 percent, these forces are greatly reduced so that the snow deposit, is shed because of aerodynamic and gravitational forces.

In Poots and Skelton (1994a), approximate analytical models for the prediction of LWC for axial and cylindrical sleeve growth were presented. These models are based on the earlier thermodynamic model of Grenier et al. (1986) for the prediction of LWC during cylindrical sleeve growth. In the analytical studies, the large relaxation time approximation of Poots and Rodgers (1976) was invoked, namely that the trajectory paths of snowflakes are rectilinear (see Wakahama et al. 1977). During axial growth, when a snow root exists on the conductor, the conductor can be either thermally insulated, thus playing no part in the heat balance for the determination of the LWC, or it can transfer heat from the warm air to the snow root by conduction.

It is the purpose of this paper to present a numerical study of thermodynamic models for the prediction of LWC during axial growth on a fixed conductor. For a range of meteorological conditions yielding temporal limiting values of the LWC (say 40 percent), critical cohesive "precipitation—air temperature" criteria are established that control wet-snow shedding and provide quantitative information on the transient sawtooth wet-snow loading of overhead line conductors, as observed in field measurements. This two-dimensional (2-D) numerical study is relevant to the prediction of LWC on a conductor of finite span and finite torsional stiffness, thus accounting for the effects of conductor rotation and the progressive formation of cylindrical sleeve growth across the span of the conductor. The first step in the construction of thermodynamic models of LWC during axial growth is to list the approximations invoked. These are as follows:

(1) It is assumed that snowflakes are at the fusion temperature T_F and possess the following liquid water content:

$$\gamma = 0.04 T_a^2 \tag{1}$$

for air temperature $T_a \in [0, 5]^\circ$C, (see field studies of conditions in Japan and France by Admirat et al. 1988b).

(2) It is assumed that the snowflake fragment adhering on impact contributes to the growth rate at the point of impact.

Address reprint requests to G. Poots, Centre for Industrial Applied Mathematics, University of Hull, HU6 7RX, Hull, UK.

Received 2 May 1994; accepted 18 August 1994

Int. J. Heat and Fluid Flow 16: 43–49, 1995

655 Avenue of the Americas, New York, NY 10010

0142-727X/95/$10.00
SSDI 0142-727X(94)00007-Y

The accretion factor σ, or proportion of snowflake mass that adheres after impact, is either taken as constant in the following global form:

$$\sigma = \sigma_0 \tag{2}$$

or in the following local form:

$$\sigma = \sigma_0 \cos\phi \tag{3}$$

where ϕ is the angle between the snowflake trajectory and the normal to the surface at the point of impact, namely

$$\phi = \cos^{-1}\left(\frac{\mathbf{v}_f \cdot \mathbf{n}}{|\mathbf{v}_f|}\right) \tag{4}$$

and $\mathbf{v}_f$ is the snowflake velocity vector, and $\mathbf{n}$ is the outward unit normal to the surface.

Numerical and analytical (LRTA) solutions of the nonlinear evolution equation for wet-snow accretion, assuming cosine law (Equation 4) for snowflake adhesion, are available in Poots and Skelton (1994b); these theoretical solutions predict snow profiles in exact agreement with the field observations of Tunstall and Koutselos (1986).

In general,

$$\sigma_0 = \sigma_0(r_0;\, U,\, G,\, T_a,\, Hr) \tag{5}$$

is a function of the conductor radius $r_0(m)$ and the meteorological variables: wind speed $U(\mathrm{m\,s^{-1}})$; liquid water content of the air $G = P/(3600 \times v_T)(\mathrm{kg\,m^{-3}})$, where $v_T(\mathrm{m\,s^{-1}})$ is the terminal speed of an average sized snowflake at precipitation rate $P(\mathrm{mm(H_2O)\,h^{-1}})$; relative humidity Hr. To date, Sakamoto and Miura (1993) have established that the accretion factor decreases as the wind speed increases, achieving a maximum value in the air temperature range $T_a \in [0, 2]^\circ\mathrm{C}$.

(3) Theoretical relationships for the density of wet snow, as a function of the meteorological parameters U, P, T_a, Hr, are not available. In a thermodynamic simulation of wet-snow accretion on a conductor under wind-tunnel conditions, the observations of Sakamoto et al. (1988) show that the density of the snow sleeve increases with increasing wind speed, increasing the precipitation rate delays metamorphosis (decreasing the density), while increasing the air temperature transforms ice crystals into spherical granules, yielding a more compact snow matrix (increasing the density). From field measurements in Japan and France by Admirat et al. (1988b), the recommended density relationship for France is as follows:

$$\rho_s = (100 + 20U)(\mathrm{kg\,m^{-3}}) \tag{6}$$

and this relationship is assumed in the present investigation.

(4) It is assumed that the snow matrix is at fusion temperature T_F.

(5) The physical properties of wet snow are currently under investigation. In particular, in the measurement of LWC, Brun et al. (1988) report that it is difficult to collect a homogeneous snow sample at a specified value of the LWC. Moreover, it is observed that the LWC of the snow matrix for snow accreted on a conductor is not uniformly distributed, especially when the density of the accreted snow is relatively low ($\rho_s < 400\,\mathrm{kg\,m^{-3}}$) (see Sakamoto et al. 1988). Thermodynamic models of LWC in accreted wet snow on conductors are based on a global energy balance for the snow/air and snow root surfaces. Consequently, in the theoretical models of Grenier et al. (1986) and Admirat et al. (1988a), the accretion process is assumed to be quasi-steady, and the models predict a mean value for the LWC. It is further assumed that the ice/water composition of the air/snow surface can be deduced using the mean value for the LWC.

The next step in the construction of the thermodynamic model is to identify the heat and mass transfer processes in the

Notation

Bi	Biot number for conductor
c_a	specific heat of air, $\mathrm{J\,kg^{-1}K^{-1}}$
c_0	specific heat of conductor, $\mathrm{J\,kg^{-1}\,K^{-1}}$
e_i	saturation vapour pressure over ice, kPa
e_w	saturation vapor pressure over water, kPa
G	liquid water content per unit volume of air, $\mathrm{kg\,m^{-3}}$
$\bar{h}$	average surface heat transfer coefficient, $\mathrm{W\,m^{-2}K^{-1}}$
H_0	atmospheric pressure, kPa
Hr	relative humidity
K_a	thermal conductivity of air, $\mathrm{W\,m^{-1}K^{-1}}$
K_0	thermal conductivity of conductor, $\mathrm{W\,m^{-1}K^{-1}}$
L_E	latent heat of evaporation, $\mathrm{J\,kg^{-1}}$
L_F	latent heat of fusion, $\mathrm{J\,kg^{-1}}$
L_S	latent heat of sublimation, $\mathrm{J\,kg^{-1}}$
M	snow load per unit length, $\mathrm{kg\,m^{-1}}$
$\mathbf{n}$	outward normal on snow surface
$\mathbf{n}_0$	outward normal on conductor surface
Nu	Nusselt number
P	snow precipitation rate, $\mathrm{mm(H_2O)\,h^{-1}}$
q	dimensionless heat flux
Q	heat flux, $\mathrm{W\,m^{-2}}$
r	radial polar coordinate, m
R	dimensionless radial polar coordinate
Re	Reynolds number for conductor
r_0	radius of conductor, m
s	perimeter of snow surface, m
t	time, s
T	dimensionless accretion time
T_a	ambient air temperature, °C
T_F	fusion temperature, °C
T_0	conductor temperature, °C
U	wind speed, $\mathrm{m\,s^{-1}}$
$\mathbf{v}_f$	velocity of average sized snowflake, $\mathrm{m\,s^{-1}}$
v_T	terminal speed of average sized snowflake, $\mathrm{m\,s^{-1}}$
(x, y)	Cartesian coordinates, m

Greek symbols

γ	LWC of snowflake
η_a	viscosity of air, $\mathrm{Nsm^{-2}}$
θ	angular polar coordinate
θ_0	angular location of upper grazing trajectory
Θ	dimensionless temperature of conductor
Λ	LWC of snow matrix
ν_a	kinematic viscosity of air, $\mathrm{m^2\,s^{-1}}$
ρ_a	density of air, $\mathrm{kg\,m^{-3}}$
ρ_s	density of snow matrix, $\mathrm{kg\,m^{-3}}$
σ	accretion factor
τ	dimensionless time in cooling period
ϕ	angle of impact
χ_i	heat transfer parameter for ice
χ_w	heat transfer parameter for water

early stages of snowflake impaction. When the conductor surface is insulated, there is no problem because accretion can take place instantaneously on snowflake impact. In general, at the onset of the snow storm, the conductor temperature $T_0 = T_a$ and hence accretion cannot take place on the windward face of the conductor until the surface has cooled down to $T_F = 0°C$. The mechanism for this cooling, which takes place on the conductor surface (or snow root) between the location of the grazing trajectories of an average sized snowflake, is to assume that if $T_0 > T_F$, all of the adhering snow melts. It is further assumed that accretion cannot take place on the snow root surface until this part of the conductor surface is at fusion temperature. This latter assumption is equivalent to the assumption that the conductor has reached a steady-state temperature before accretion can commence.

In the next section, the cooling down process of the windward face of the conductor is formulated. Employing a heat balance to supplement the equations governing the evolution of the snow surface, a differential equation for the prediction of the mean value of the LWC for the snow matrix is formulated. Then follows a section on results on LWC for different thermodynamic models, giving some preliminary thoughts to a quantitative understanding of snow shedding in relation to LWC.

Cooling of the windward face of the conductor

The thermal response of the conductor, caused by heat loss on the melting of adhering snowflake fragments and by evaporation at the resulting wet surface, is governed by the following equations (see Figure 1):

$$K_0 \nabla^2 T_0 = \rho_0 c_0 \frac{\partial T_0}{\partial t}, \quad r < r_0, \quad \theta \in [0, 2\pi] \tag{7}$$

subject to the following initial condition:

$$T_0 = T_a, \quad r \leq r_0, \quad t = 0 \tag{8}$$

and for $t > 0$ on the snow-root surface $\mathscr{C}_1$: $r = r_0$, $\theta \in [\theta_0, 2\pi - \theta_0]$,

$$K_0 \nabla T_0 \cdot \mathbf{n}_0 = \bar{h}(T_a - T_0) - (1 - \gamma) G(-\mathbf{v}_f \cdot \mathbf{n}_0) L_F - \chi_w \Delta e_w \tag{9}$$

and on the conductor/air surface $\mathscr{C}_0$: $r = r_0$, $\theta \in [0, \theta_0]$, and $\theta \in [2\pi - \theta_0, 2\pi]$,

$$K_0 \nabla T_0 \cdot \mathbf{n}_0 = \bar{h}(T_a - T_0) \tag{10}$$

In the system of Equations 7–10 K_0(W m^{-1}K^{-1}), ρ_0(kg m^{-3}), and c_0(J kg^{-1}K^{-1}) denote the thermal conductivity, density, and specific heat of the conductor, respectively; $\bar{h}$(W m^{-1}K^{-1}) is an average surface heat transfer coefficient for the system; L_F(J kg^{-1}) is the latent heat of melting ice; $e(T)$(kPa) is the saturation vapour pressure at temperature T; $\mathbf{n}_0$ is the unit vector normal to the conductor suface; and in polar coordinates (r_0, θ_0) is the location of the upper grazing trajectory of an average sized snowflake.

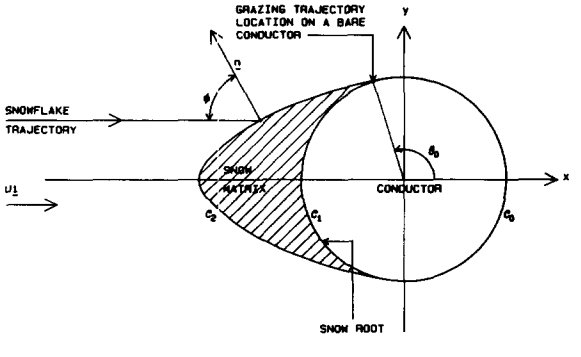

Figure 1 Schematic diagram of wet-snow impaction

In the heat balance (Equation 9) for heat loss at the snow-root, the deficit in saturation pressure over water is as follows:

$$\Delta e_w = e_w(T_a) - e_w(T_F) \tag{11}$$

Polynomial expressions for the saturation pressure e_w (over water) are available in Lowe (1977), and, moreover, application of the heat and mass transfer analogy of Chilton and Colburn (1934) yields the following:

$$\chi_w = 0.622 \bar{h} L_E Hr / c_a H_0 l^{2/3} \tag{12}$$

where L_E(J kg^{-1}) is the latent heat of evaporation of water; c_a(J kg^{-1}K^{-1}) is the specific heat of air; H_0(kPa) is the air pressure; and $l = 0.875$ is the Lewis number. Szilder et al. (1988) provide heat transfer data relevant to snow cylinders in the form of the following average heat transfer coefficient:

$$\bar{h} = \overline{\mathrm{Nu}} K_a / 2r_0 \tag{13}$$

The length scale of the accretion was taken as the diameter $2r_0$ of the conductor and recommended values of the average Nusselt number $\overline{\mathrm{Nu}}$ are given as follows:

$$\overline{\mathrm{Nu}} = 0.117 \mathrm{Re}^{0.68}, \quad \mathrm{Re} = 2r_0 U / v_a \tag{14}$$

for the Reynolds number range $\mathrm{Re} \in [(1.5 \times 10^4), (1.7 \times 10^5)]$. In the above, K_a(W m^{-1}K^{-1}) and v_a(m^2 s^{-1}) are the thermal conductivity and kinematic viscosity of air, respectively.

Let the steady-state temperature distribution for the cooling down period be reached at time $t = t_0$; this is taken to be the time at which the mean value of the temperature over the snow-root surface is $T_0 = 0.01°C$, say. Thus, for $t > t_0$, it is assumed that a steady-state temperature exists within the conductor because the snow root is now covered with wet snow at $T_F = 0°C$. Further details concerning the solution of the above heat conduction problems and the evaluation of the heat flux at the snow root for $t > t_0$ are given in the Appendix.

Determination of LWC during wet-snow accretion

In Poots and Skelton (1994a) a differential equation was formulated for determining the LWC for the two limiting modes of accretion; namely, axial growth and cylindrical sleeve growth. On assuming that the accretion factor $\sigma = \sigma_0$ (constant) and that snowflake trajectories are rectilinear (LRTA), analytical solutions were presented. It is known that the collection efficiency of the wet-snow profile decreases with time, so a numerical study for the prediction of LWC is undertaken. In the following, numerical solutions for the accretion process (see Skelton and Poots 1991 and Poots and Skelton 1994b) are employed to predict LWC, assuming σ is given by Equations 2 and 3; for completeness, in the case of $\sigma = \sigma_0 \cos \phi$, analytical solutions for the LWC are obtained on using the LRTA analytical predictions for wet-snow growth, as given in Poots and Skelton (1994b).

The liquid water content of the snow matrix is denoted by Λ. The net increase in liquid water content is attributable to the melting snow matrix by snow surface heat transfer (air and root surfaces $\mathscr{C}_2$ and $\mathscr{C}_1$, respectively); this is given by $(\Lambda - \gamma)M(t)$, where $M(t)$ is the mass of wet snow deposited during time t. Heat is gained by the snow matrix by convective

heat transfer at the snow/air surface.

$$Q_2 = \bar{h}(T_a - T_F)s \tag{15}$$

where s is the perimeter of the snow surface $\mathscr{C}_2$ (see Figure 1). Heat lost by evaporation and sublimation at the snow/air boundary $\mathscr{C}_2$ is given by the following:

$$Q_3 = [(1 - \Lambda)\chi_i \Delta e_i + \Lambda \chi_w \Delta e_w]s \tag{16}$$

see assumption (5). Here, the deficit in saturation pressure over ice is as follows:

$$\Delta e_i = e_i(T_a) - e_i(T_F) \tag{17}$$

and

$$\chi_i = 0.622\bar{h}L_S Hr/c_a H_o l^{2/3} \tag{18}$$

where L_s(J kg^{-1}) is the latent heat of sublimation.

The rate of production of melt water within the snow matrix is given by the following:

$$L_F \frac{\mathrm{d}}{\mathrm{d}t}[(\Lambda - \gamma)M(t)] = Q_1 + Q_2 - Q_3 \tag{19}$$

where Q_1, Q_2, and Q_3 are given by A8–A9, A15, and A16, respectively. Following Poots and Skelton (1994a), introduce the following dimensionless accretion time

$$T = \sigma_0 GUt/\rho_s r_0 \tag{20}$$

and the (convenient) dimensionless heat transfer groups

$$\delta = \{\bar{h}(T_a - T_F) - \chi_i \Delta e_i\}/\sigma_0 GUL_F \tag{21}$$

$$\varepsilon = -\{\chi_w \Delta e_w - \chi_i \Delta e_i\}/\sigma_0 GUL_F \tag{22}$$

$$\alpha = \bar{h}(T_a - T_F)/\sigma_0 GUL_F \tag{23}$$

The governing equation for the LWC transforms to the following:

$$\frac{d}{dt}\left[(\Lambda - \gamma)\frac{M(T)}{\rho_s r_0^2}\right] = \alpha q_1 + (\delta + \Lambda\varepsilon)\frac{s}{r_0} \tag{24}$$

and depends upon the accretion kinetics: the dimensionless snow load $M(T)/\rho_s r_0^2$, the dimensionless snow/air perimeter length s/r_0, and the dimensionless heat flux q_1 at the snow root (defined in the Appendix). If the accretion process commences at $T \equiv \sigma_0 GU(t - t_0)/\rho_s r_0 = 0$, the initial condition for the solution of Equation 24 is as follows:

$$\Lambda(0) = \gamma[(\dot{M}(0)/\rho_s r_0^2) + \alpha q_1 + \delta(s(0)/r_0)]/ [\dot{M}(0)/\rho_s r_0^2 - \varepsilon(s(0)/r_0)] \tag{25}$$

where the overdot denotes d/dT. Initially the dimensionless snow/air perimeter is

$$s(0)/r_0 = 2(\pi - \theta_0) \tag{26}$$

and the rate of mass accretion is evaluated from the mass transfer balance

$$\frac{\dot{M}(0)}{\rho_s r_0^2} = \int_{\theta_0}^{2\pi - \theta_0} \frac{\sigma}{\sigma_0}\left(-\frac{\mathbf{v}_f}{U}\cdot \mathbf{n}_0\right) d\theta \tag{27}$$

Numerical solution of the LWC equation

The input functions $M(T)/\rho_s r_0^2$ and $s(T)/r_0$ are complex functions of T and, in general, are available on the numerical solution of the system of nonlinear partial differential equations that govern the snow-accretion kinetics (see Skelton and Poots 1991). For this reason, the LWC Equation 24, subject to Equation 25, is solved by standard predictor–corrector methods. Procedures for the calculation of $M(T)/\rho_s r_0^2$ and $s(T)/r_0$ are available in Skelton and Poots (1991) for accretion factor $\sigma = \sigma_0$, and in Poots and Skelton (1994b), for the cosine law accretion factor $\sigma = \sigma_0 \cos\phi$. Illustrations of the transient behaviour of the LWC during accretion and its sensitivity with respect to meteorological parameters are now discussed.

Results and Discussion

The physical properties of the snow/conductor system are listed in Table 1. Properties of the average sized snowflake, such as snowflake mass, snowflake size, and snowflake drag coefficient, as a function of meteorological conditions, are available in Skelton and Poots (1991). Therefore, as to present illustrations in real time, the accretion constant σ_0, given in Equation 5, is taken as unity. Its actual value for UK meteorological conditions remains to be determined on calibration of the wet-snow predictions of the theoretical model with field measurements, historical weather, and snow-load data.

For a constant accretion factor σ_0, the LWC is displayed in Figure 2 for a 2-hour snow storm for which $T_a = 1°C$, $P = 1.0$ mm(H_2O) h^{-1}, $U = 5$ m s^{-1}, and $Hr = 0.95$. When the conductor is thermally insulated, so that at the snow root $q_1 = 0$ in Equation 24, there is excellent agreement between the values of the LWC calculated using the numerical method compared with the analytical solution based on the LRTA (see Poots and Skelton 1994a). When the conductor is noninsulated, so that heat is transferred by conduction from the warm air to the snow root ($q_1 \neq 0$), the agreement between predicted values of the LWC using the numerical and analytical models are within 4 percent at the end of the 2-hour period. Note that, in these models, the effect of heat transfer across the conductor is to cause a significant increase in the LWC. Moreover, it has been established that the effects of varying meteorological parameters T_a, P, and U on the LWC for the insulated conductor are not appreciable; therefore, in the following, the discussion concentrates mainly on the more realistic case of the noninsulated conductor.

Table 1 Physical properties

		Conductor	Air
Density	ρ, kg m^{-3}	2.937×10^3	1.3
Specific heat	c, J kg^{-1}k^{-1}	9.0×10^2	1.006×10^3
Thermal conductivity	K, W m^{-1}K^{-1}	4.0	2.42×10^{-2}
Radius of conductor	r_0, m	1.863×10^{-2}	—
Kinematic viscosity	v, m^2 s^{-1}	—	1.36×10^{-5}
Latent heat of evaporation	L_E, J kg^{-1}	2.51×10^6	
Latent heat of fusion	L_F, J kg^{-1}	3.25×10^5	
Latent heat of sublimation	L_S, J kg^{-1}	2.835×10^6	

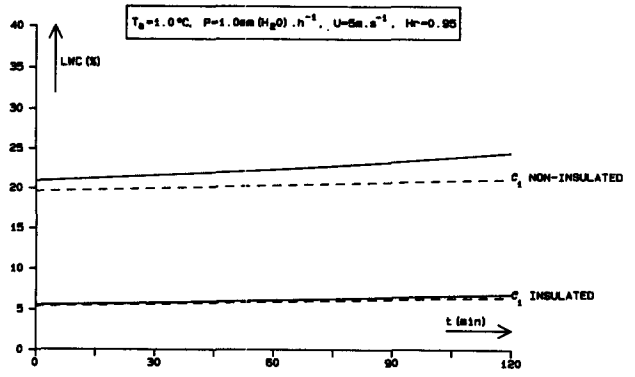

Figure 2 Liquid water content (LWC) of snow deposit for constant accretion factor; solid line, numerical; dashed line, analytical

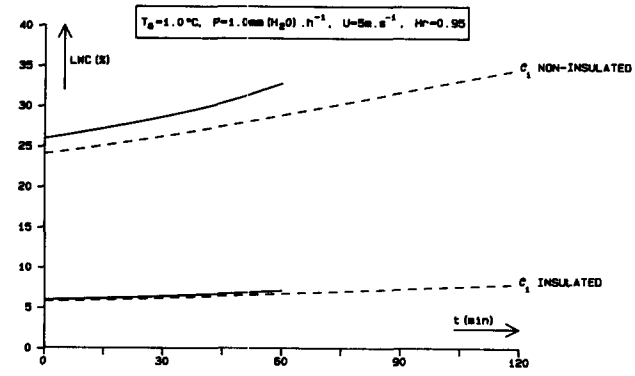

Figure 3 LWC of snow deposit for cosine law accretion factor; solid line, numerical; dashed line, analytical

In Figure 3, predictions for the LWC are given for the cosine law accretion factor $\sigma = \sigma_0 \cos \phi$; the duration and meteorological variables for the snow storm are as in Figure 2. In this case, the numerical model is known to develop numerical instabilities after the first hour; the reason is that the radius of curvature of the snow profile at the stagnation line rapidly tends to zero with increasing time. For the insulated conductor, as in Figure 2, the agreement between the LWC calculated using the numerical and analytical models is excellent; here, use of the term "analytical model" is to indicate that analytical solutions are known (see Poots and Skelton 1994b), for the wet-snow accretion kinetics for all time. For the noninsulated conductor the difference in predictions for LWC in the first hour using the numerical and analytical models is, again, more pronounced than for the insulated conductor. In the numerical model, both the mass of snow accreted and the perimeter of the air/snow surface are less than in the analytical model (LRTA). However, the heat flux into the snow root $\theta \in (\theta_0, 2\pi - \theta_0)$ for the numerical model is greater than for the analytical model $\theta \in (\pi/2, 3\pi/2)$, and it is this latter feature that dictates the difference in LWC between the two models. In the numerical model, the LWC is 26 percent initially, increasing in just one hour to a critical level of 33 percent, at which snow shedding may occur.

The analytical model for the cosine law of accretion is used to illustrate the effects of varying the meteorological conditions T_a, P, U, and Hr, see Figure 4(a,b,c). Figures 4(a), for $P = 1.0\,\text{mm}(H_2O)\,h^{-1}$, $U = 5\,\text{m}\,s^{-1}$, and $Hr = 0.95$, shows, for a 2-hour period, the increase in LWC due to increasing the air temperature T_a; clearly, for $T_a = 2.5°C$, the LWC reaches

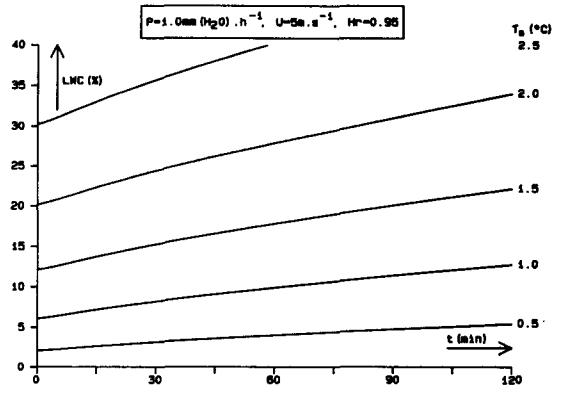

Figure 4(a) LWC of snow deposit for various air temperatures using the analytical model for the cosine law

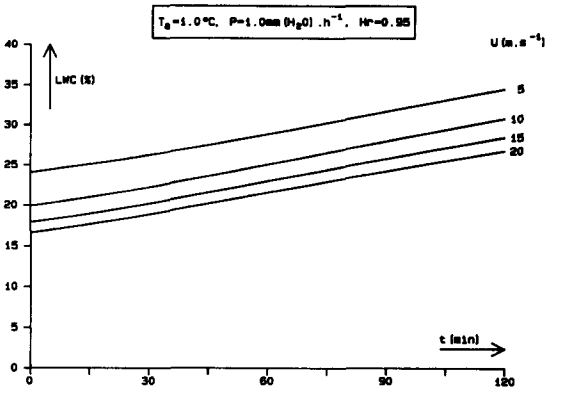

Figure 4(b) LWC of snow deposit for various wind speeds using the analytical model for the cosine law

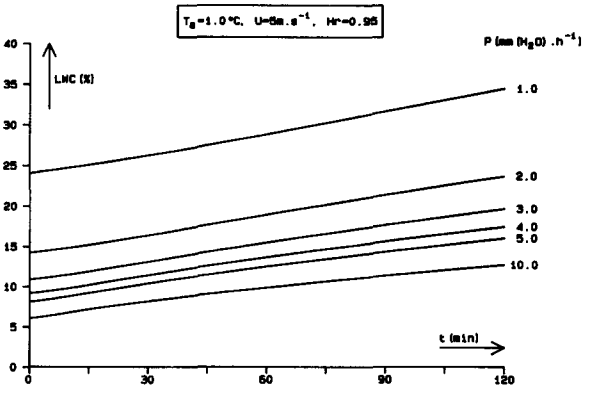

Figure 4(c) LWC of snow deposit for various precipitation rates using the analytical model for the cosine law

40 percent in the first hour and, in this context, it should be remembered (see Figure 3) that the LWC is always underestimated by the analytical model. In Figure 4(b), for $T_a = 1°C$, $P = 1.0\,\text{mm}(H_2O)\,h^{-1}$, and $Hr = 0.95$, it is seen that the effect of increasing the wind speed is to decrease the LWC. Finally, in Figure 4(c), a similar trend is established, for $T_a = 1°C$, $U = 5\,\text{m}\,s^{-1}$, and $Hr = 0.95$, when the precipitation rate P is increased. In conclusion, a rise in air temperature, as expected, raises the LWC while LWC is decreased when either the wind speed or precipitation is increased.

It is now understood that the LWC of the snow deposit controls its mechanical cohesion. When LWC increases, the internal cohesive forces (capillary force, ice bonding) decrease, and for some maximum size of deposit, the external aerodynamic and gravitational forces overcome the internal forces so that the snow sleeve breaks up or separates from the conductor. This relationship between maximum size and LWC is not understood: all that is known is that the maximum size adhering to the conductor decreases rapidly as LWC increases (see Admirat et al. 1988a). In Figure 5, the cohesive $(P - T_a)$ limits are given for a LWC of 40 percent at the onset of accretion and at the end of a 1-hour period. Thus, for a fixed air temperature T_a and a fixed wind velocity U, the cohesive $(P - T_a)$ limits give the critical value of P_c to yield LWC = 40 percent: if $P > P_c$, accretion will continue; whereas, if $P < P_c$, LWC > 40 percent, and, by implication, the deposit is shed.

Knowing the critical value of the precipitation rate P for fixed T_a, U, the corresponding mass $M(T_a, P, U, t)$ can be computed; equally well, the size of the accretion represented by the axial length of the deposit, measured from the snow root to the forward stagnation line, can be deduced, if required. In Figure 6 the snow load corresponding to the cohesive $(P - T_a)$ limits is shown for 40 percent LWC existing at the end of a 1-hour snow storm; the critical snow load increases with increasing wind speed.

It is assumed, once the 40 percent LWC level is reached, that the snow deposit is shed, then the transient snow

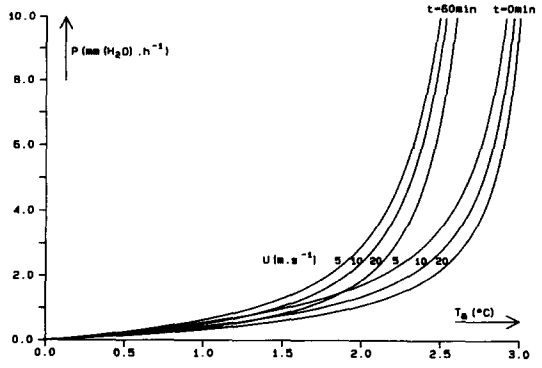

Figure 5 Cohesive $(P - T_a)$ limits for LWC of 40 percent at $t = 0$ and $t = 60$ min using the analytical model for the cosine law

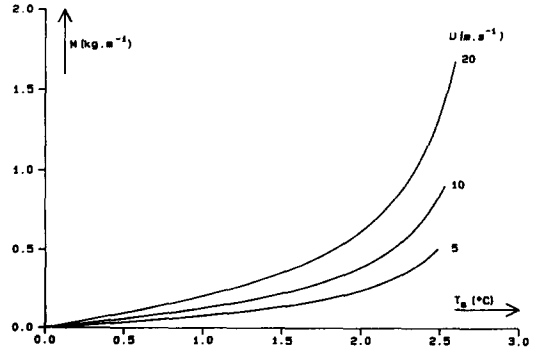

Figure 6 Snow load corresponding to cohesive $(P - T_a)$ limits at $t = 60$ min for LWC of 40 percent using the analytical model for the cosine law

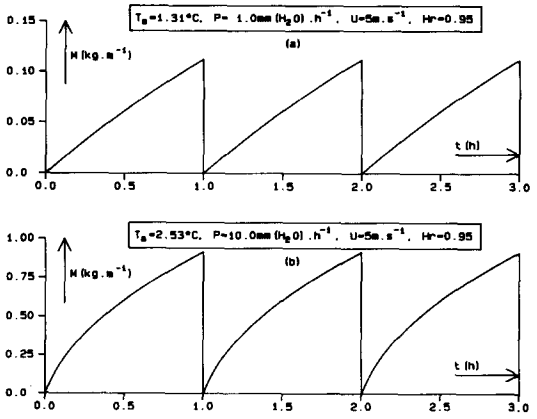

Figure 7 Snow load: accretion and shedding at LWC of 40 percent using the analytical model for the cosine law: (a) (T_a, P, U, Hr) = (1,31, 1.0, 5, 0.95); (b) (T_a, P, U, Hr) = (2.53, 10.0, 5, 0.95)

loading on the conductor will be of the sawtooth form. Some preliminary results illustrating this form of wet-snow growth are given in Figures 7(a,b), respectively, for the two critical cases at one-hour: $(P, T_a, U, Hr) = (1.0, 1.31, 5.0, 0.95)$ and (10.0, 2.53, 5.0, 0.95). In this way the thermodynamic model for the prediction of LWC during axial growth can provide useful quantitative information on wet-snow shedding.

For a conductor of finite span and finite torsional stiffness, it is known that conductor rotation, caused by snow and aerodynamic torques (see Skelton and Poots 1991), controls the extent of snow loading and its mode of growth across the span (axial growth near the tower changing progressively to cylindrical sleeve growth at the center of the span). The results of the present 2-D, time-dependent study of LWC during axial growth underlines the dependence of wet-snow growth and shedding on this thermodynamic variable. These results should prove useful on undertaking a three-dimensonal (3-D), time-dependent study of snow load and LWC across a conductor span.

Conclusion

Thermodynamic models have been developed for the prediction of the LWC of the snow matrix during axial growth of wet snow on a fixed conductor. Results have been obtained by numerical and analytical methods for the accretion factor taken as a constant or for the accretion factor obeying a cosine law, the latter being postulated so as to predict snow profiles in agreement with the UK field observations of Tunstall and Koutselos (1986). Preliminary results of critical cohesive "precipitation–air temperature" limits are obtained for the LWC level of 40 percent, indicating snow shedding. Quantitative information is also given on the role of the thermodynamic variable LWC on sawtooth growth during wet-snow accretion.

Acknowledgment

The authors are indebted to the National Grid Company for supporting this research, which is published by permission of the National Grid Company.

References

Admirat, P., Maccagnan, M. and De Goncourt, B. 1988a. Influence of Joule effect and of climate conditions on liquid water content of snow accreted on conductors. *Proc. Fourth Int. Conf. on Atmospheric Icing of Structures*, Paris, 367–370

Admirat, P., Sakamoto, Y. and DeGoncourt, B. 1988b. Calibration of snow accumulation model based on actual cases in Japan and France. *Proc. Fourth Int. Conf. on Atmos. Icing of Structures*, Paris, 129–133

Brun, E., Panel, J. M. and Lafeuille, J. 1988. Dielectric measurements of snow liquid water content. *Proc. Fourth Int. Conf. on Atmos. Icing of Structures*, Paris, 287–290

Chilton, T. J. and Colburn, M. P. 1934. Mass transfer coefficients. *Ind. Eng. Chem.*, **26**, 1183–1187

Grenier, J. C., Admirat, P. and Maccagnan, M. 1986. Theoretical study of the heat balance during the growth of wet-snow sleeves on electrical conductors. *Proc. Third Int. Conf. on Atmos. Icing of Structures*, Vancouver, 125–128

Lowe, P. R. 1977. An approximating polynomial for the computation of saturation vapour pressure. *J. App. Met.*, **16**, 100–103

Poots, G. and Rodgers, G. G. 1976. The icing of a cable. *J. Inst. Math. Appl.*, **18**, 203–217

Poots, G. and Skelton, P. L. I. 1994a. Simple models for wet-snow accretion on transmission lines: Snow load and liquid water content. *Int. J. Heat Fluid Flow*, **15**(5), 411–417

Poots, G. and Skelton, P. L. I. 1994b. An analytical solution of a nonlinear evolution equation for wet-snow accretion: Snow load on overhead lines and aerial warning balls. *Math. Eng. Ind.*, to appear

Sakamoto, Y., Admirat, P., Lapeyre, J. L. and Maccagnan, M. 1988. Thermodynamic simulation of wet-snow accretion under wind tunnel conditions. *Proc. Fourth Int. Conf. on Atmos. Icing of Structures*, Paris, 180–185

Sakamoto, Y., and Miura, A. 1993. Comparative study of wet snow models for estimating snow load on power lines based on general meteorological parameters. *Proc. Sixth Int. Conf. on Atmos. Icing of Structures*, Budapest, 133–138

Skelton, P. L. I. and Poots, G. 1991. Snow accretion on overhead line conductors of finite torsional stiffness. *Cold Reg. Sci. Tech.*, **19**, 301–316

Smith, G. D. 1965. *Numerical Solution of Partial Differential Equations.* Oxford Mathematical Handbooks, Oxford

Sneddon, I. N. 1966. *Mixed Boundary Value Problems in Potential Theory.* Wiley, New York

Szilder, K., Waskiewicz, M. and Lozowski, E. P. 1988. Measurement of the average convective heat transfer coefficient and the drag coefficient for icing shaped cylinders. *Proc. Fourth Int. Conf. on Atmos. Icing of Structures*, Paris, 147–151

Tunstall, M. and Koutselos, L. 1986. Collection and reproduction of natural ice shapes on overhead line conductors and measurement of their aerodynamic characteristics. *Proc. Third Int. Conf. on Atmos. Icing of Structures*, Vancouver

Wakahama, G., Kuroiwa, D. and Goto, K. 1977. Snow accretion on electric wires and its prevention. *J. Glaciology*, **19**, 479–487

Appendix. Cooling of the windward surface of the conductor, heat flux at the snow root

Introducing the dimensionless variables

$$\mathbf{R} = \frac{\mathbf{r}}{r_0}, \quad \mathbf{V}_f = \frac{\mathbf{v}_f}{U}, \quad \tau = \frac{K_0 t}{\rho_0 c_0 r_0^2}, \quad \Theta = \frac{T_0 - T_F}{T_a - T_F} \tag{A1}$$

the governing Equations (7–10) transform to the following:

$$\bar{\nabla}^2\Theta = \frac{1}{R}\frac{\partial}{\partial R}\left(R\frac{\partial\Theta}{\partial R}\right) + \frac{1}{R^2}\frac{\partial^2\Theta}{\partial\theta^2} = \frac{\partial\Theta}{\partial\tau} \tag{A2}$$

subject to the following conditions:

$$\Theta(R, \theta, 0) = 1, \quad R \le 1, \quad \theta \in (0, 2\pi) \tag{A3}$$

for $\tau > 0$ on the root surface $\mathscr{C}_1$: $R = 1$, $\theta \in (\theta_0, 2\pi - \theta_0)$

$$\frac{\partial\Theta(1,\theta)}{\partial R} = \mathrm{Bi}[1 - \Theta(1, \theta, \tau)] - q_0 \tag{A4}$$

for $\tau > 0$ on the bare conductor $\mathscr{C}_0$: $R = 1$, $\theta \in (0, \theta_0)$, and $\theta \in (2\pi - \theta_0, 2\pi)$

$$\frac{\partial\Theta(1,\theta)}{\partial R} = \mathrm{Bi}[1 - \Theta(1, \theta, \tau)]. \tag{A5}$$

Here the conductor Biot number and the dimensionless heat flux are defined, respectively, by the following:

$$\mathrm{Bi} = \bar{h}r_0/K_0, \quad q_0 = \frac{r_0[(1-\gamma)(-G\mathbf{V}_f\cdot\mathbf{n}_0)L_F + \chi_w\Delta e_w]}{K_0(T_a - T_F)} \tag{A6}$$

For $\tau > \tau_0 = K_0 t_0/\rho_0 c_0 r_0^2$, the steady-state mixed Dirichlet–Neumann problem to be solved is as follows:

$$\bar{\nabla}^2\Theta = 0 \tag{A7}$$

subject to the condition $\Theta(1, \theta) = 0$ on $\mathscr{C}_1$ and the condition A5 on $\mathscr{C}_0$. The above mixed Dirichlet–Neumann problems cannot be solved analytically (see Sneddon 1966), but are readily solved numerically by standard finite difference methods described in Smith (1965).

For $t > t_0$, the heat flux at the snow root $\mathscr{C}_1$ into the snow matrix is as follows:

$$Q_1 = -K_0(T_a - T_F)\int_{\theta_0}^{2\pi-\theta_0}\frac{\partial\Theta(1,\theta)}{\partial R}\,\mathrm{d}\theta \tag{A8}$$

Application of the divergence theorem to Equation A7 yields the following:

$$Q_1 = \bar{h}r_0(T_a - T_F)q_1, \quad q_1 = \int_{\theta_0}^{2\pi-\theta_0}[1 - \Theta(1, \theta)]\,\mathrm{d}\theta \tag{A9}$$